Molecular BioSystems

PAPER

View Article Online
View Journal | View Issue

Cite this: *Mol. BioSyst.*, 2015, 11, 2008

^{1}H NMR brain metabonomics of scrapie exposed sheep

Paola Scano,*[a] Antonella Rosa,[b] Alessandra Incani,[b] Caterina Maestrale,[c] Cinzia Santucciu,[c] Daniela Perra,[b] Sarah Vascellari,[b] Alessandra Pani[b] and Ciriaco Ligios[c]

While neurochemical metabolite modifications, determined by different techniques, have been diffusely reported in human and mice brains affected by transmissible spongiform encephalopathies (TSEs), this aspect has been little studied in the natural animal hosts with the same pathological conditions so far. Herein, we investigated, by high resolution ^{1}H NMR spectroscopy and multivariate statistical data analysis, the brain metabolite profile of sheep exposed to a scrapie agent in a naturally affected flock. On the basis of clinical examinations and western blotting analysis for the pathological prion protein (PrP^{Sc}) in brain tissues, sheep were catalogued as not infected (H), infected with clinical signs (S), and infected without clinical signs (A). By discriminant analysis of spectral data, comparing S *vs.* H, we found a different metabolite distribution, with inosine, cytosine, creatine, and lactate being higher in S than in H brains, while the branched chain amino acids (leucine, isoleucine, and valine), phenylalanine, uracil, tyrosine, gamma-amino butyric acid, total aspartate (aspartate + *N*-acetyl aspartate) being lower in S. By a soft independent modelling of class analogy approach, 1 out of 3 A samples was assigned to class H. Furthermore, A brains were found to be higher in choline and choline-containing compounds. By means of partial least squares regression, an excellent correlation was found between the PrP^{Sc} amount and the ^{1}H NMR metabolite profile of infected (S and A) sheep, and the metabolite mostly correlated with PrP^{Sc} was alanine. The overall results, obtained using different chemometric tools, were able to describe a brain metabolite profile of infected sheep with and without clinical signs, compared to healthy ones, and indicated alanine as a biomarker for PrP^{Sc} amounts in scrapie brains.

Received 17th February 2015,
Accepted 20th April 2015

DOI: 10.1039/c5mb00138b

www.rsc.org/molecularbiosystems

Introduction

Scrapie is a fatal neurodegenerative disease that affects sheep and goats. This disease belongs to the transmissible spongiform encephalopathies (TSEs), or prion diseases, a group of pathologic conditions that includes bovine spongiform encephalopathy (BSE) in cattle, chronic wasting disease (CWD) in deer, Creutzfeldt–Jakob disease (CJD) and variant CJD (vCJD) in humans.[1] TSEs consist of the deposition, within the central nervous system (CNS) and in a number of peripheral nervous and lymphoid tissue districts, of the pathological isoform (PrP^{Sc}) of a normal host protein ("prion protein", PrP^{c}).[1] Studies in rodent models and field observations in sheep suggested that the classical scrapie agent enters into the host's body through the mucosa of the ileal tract of the gut, with the first PrP^{Sc} deposition being observed in Peyer's patches (PPs) and then in other districts of the lymphoreticular system (LRS).[2] From the LRS, prions enter inside the CNS through the sympathetic and parasympathetic fibers of the autonomic nervous system, with the first appearance of PrP^{Sc} deposition at the level of the nucleus parasympathicus nervi vagi (NPNV) and the intermedio-lateral (IML) cell column of the thoracic spinal cord.[3] During the lymphoid spreading of PrP^{Sc} and its early phase of neurodeposition, sheep appear clinically healthy. Following a 2-year-long incubation period, onset of clinical scrapie is associated with diffuse PrP^{Sc} deposition, neuronal vacuolation, astrocytosis and microglia activation in the CNS.[1] All these changes result in complex alterations of cellular metabolites that have been studied by means of low resolution magnetic resonance spectroscopy (MRS) *in vivo* and *ex vivo* brains and tissues and by high resolution proton nuclear magnetic resonance (^{1}H NMR) in brain extracts.[4–6] In our previous work, analyzing the lipid composition in brain extracts from healthy and naturally scrapie infected sheep using different techniques, a significant enrichment of saturated fatty acids in symptomatic-sheep brains was observed, which may affect thermodynamic properties and phase behavior of neuronal membranes.[7]

"Metabonomics" has been defined as "understanding the metabolic responses of living systems to pathophysiological

[a] *Department of Chemical and Geological Sciences, University of Cagliari, Monserrato, Italy. E-mail: scano@unica.it*
[b] *Department of Biomedical Sciences, University of Cagliari, Monserrato, Italy*
[c] *Istituto Zooprofilattico Sperimentale della Sardegna, Sassari, Italy*

stimuli *via* multivariate statistical analysis (MVA) of biological NMR spectroscopic data''.[8] MVA is a powerful tool that allows us to extract qualitative and quantitative information from large data sets. Among MVA techniques, qualitative techniques such as cluster analysis, principal component analysis (PCA), and soft independent modelling of class analogy (SIMCA) are aimed at finding similarities and dissimilarities among samples. For sample classification and biomarker identification, discriminant analysis (DA) is more appropriate. Among regression techniques, partial least squares (PLS) can be used to linearly correlate multivariate data with the measured response. Multivariate statistical approaches, different from univariate tests, taking into account the correlations among variables, highlight all the concomitant changes of metabolites, thus giving a more ample picture of biomarker candidates and a more robust classification.

In this work, in an attempt to identify a metabolite profile linked to prion ailments, we studied, by means of ^{1}H NMR spectroscopy coupled with different MVA techniques, the pool of hydro-soluble low molecular weight compounds in brain extracts from Sarda breed sheep exposed to the scrapie agent in a historically affected flock. To accomplish this goal, brains were collected from healthy (H), scrapie-infected symptomatic (S), and scrapie-infected asymptomatic (A) sheep. Modifications of brain metabolite profiles were correlated with PrP^{Sc} deposition, as measured by WB analysis, in brains of the affected animals.

Material and methods

Sheep selection, scrapie diagnosis and brain treatments

A scrapie-affected Sarda sheep flock, located in Sardinia (Italy), was studied. The flock was randomly selected among those with high incidence of clinical scrapie. After notification of clinically suspect cases, inside the context of passive surveillance for scrapie, the presence of the disease in the flock was assessed by conventional protocols. In this flock, inside the framework of appropriate actions for eradicating scrapie, all the susceptible animals, with or without clinical signs, were euthanized. Whole brains were removed by standard necropsy procedures as soon as possible after death. The collected brains were divided into two hemi-parts by a medial cutting before being frozen at −80 °C. One half underwent western blotting (WB) examination[9] and PrP^{Sc} relative quantification. Eighteen brains were selected, and based on WB results they were classified as follows: n = 7, PrP^{Sc} negative, as healthy (H-1 to H-7); among 11 PrP^{Sc} positive, when clinical signs were previously reported they were classified as symptomatic (n = 8, from S-1 to S-8); otherwise asymptomatic (n = 3, from A-1 to A-3). The second half of brain was weighed and immediately homogenized in ice for 2 min in saline solution, 1 : 1 weight : volume, using an Ultra Turrax blender. Aliquots of homogenates were stored at −80 °C.

Extraction of the water-soluble low molecular weight components

For each brain, three aliquots were submitted to extraction. The low molecular weight water-soluble components were extracted from homogenized brain samples using a solution of $CHCl_3$/MeOH/H_2O (2/1/1 v/v/v) according to the Folch method.[10] Briefly, 12 mL of $CHCl_3$/MeOH was added to brain homogenates (500 mg of wet brain/mL of saline solution). After 1 h, 3 mL of H_2O was added in order to solubilize the hydrophilic components. After centrifugation at 900g for 1 h, the H_2O–MeOH mixture, containing the water-soluble low molecular weight components, was separated from the $CHCl_3$ phase that contained the lipid fraction. The water soluble phase (4 mL) was dried under rotor vacuum and redissolved in 600 μl of D_2O. From each brain, three samples were prepared for NMR analysis.

^{1}H NMR experiments

^{1}H NMR spectra were recorded at 499.839 MHz, using a Varian UNITY INOVA 500 spectrometer (Agilent Technologies, CA, USA). Experiments were carried out at 300 K, with an acquisition time of 3 s, 20 s relaxation delay, a 90° pulse, and 128 scans. For suppression of residual water resonance, a 1D NOESY pulse sequence with a mixing time of 1 ms was applied. To the free induction decay (FID), a zero-filling to 128 K and a line broadening of 0.3 Hz were applied. Chemical shifts were referred to the resonance of the standard sodium 3-trimethylsilyl-propionate-2,2,3,3-d_4 (TSP) set at 0.00 ppm. The tentative assignment of signals to metabolites was based on data reported in the literature[11–14] and with the aid of 2D NMR experiments. FID processing, manual phasing, baseline correction and area integration were performed using the MestReNova program (Version 7.1.2, Mestrelab Research S.L.).

Data pre-treatment and multivariate statistical data analysis

Spectral data pre-treatments were performed to make the samples comparable and the overall data suitable for statistical analysis. To overcome dilution problems, within each sample the integrated area of the spectral regions of interest was reported as the percentage of the total integrated areas. The resulting data matrix **X**, in which the rows are samples and columns the spectral integral values (reported as means over three spectra from as many extracts for each brain), was imported into the SIMCA-P+ program (Version 13.0, Umetrics, Sweden), and the mean was centered and scaled to unit variance, column wise. When distribution of a variable presented skewness, column wise, it was log-transformed.

The multivariate statistical approaches for data analysis employed here were as follows: (i) The unsupervised PCA for sample distribution overview, where information regarding class membership is not given; the PCA results were graphically reported in the score plots where samples were projected in the multivariate space. (ii) The supervised partial least squares-discriminant analysis (PLS-DA) and its orthogonal variant (OPLS-DA) for classification and identification of the most discriminant variables that characterized the classes. In the 2-class OPLS-DA, the between-class variance is expressed in the first component, and further orthogonal components are irrelevant to the discrimination; this is of particular interest when a high intra-class variability exist.[15] The PLS-DA model quality was evaluated on the basis of the parameters R^2Y (goodness of fit) and Q^2Y (goodness of prediction, determined through cross

validation), and tested for overfitting by permutation tests (n = 400), as implemented in the SIMCA program. The results of two OPLS-DA models can be depicted in the SUS plot (shared and unique structures plot); this is a 2D scatter plot of the loading correlation vectors of the predictive components of the two separate models.[16] (iii) The supervised classification technique soft independent modelling of class analogy (SIMCA) to classify samples as belonging to an already given class, for which they show the largest similarity. In contrast to other supervised pattern recognition techniques (PLS-DA for example), SIMCA is a more versatile approach (soft modeling), which allows the classification of a sample in one or more classes, or in none of them, while discriminant techniques (hard modelling) only allow us to classify a sample in a single class. In SIMCA, for each class of samples, a PCA is performed, where the appropriate number of principal components (PCs) to be included is based on the cross-validation procedure; in fact, although the variance explained by the PCA model (R^2X) increases with additional PCs, the analogous entity in cross-validation, expressed by Q^2X, does not continuously increase with incremental PCs, indicating, at a certain point, that the addition of more PCs into the model will only add noise. The SIMCA results are plotted as Cooman's plot, which provides the orthogonal distance from samples to be classified to two selected PCA classes. The critical cut-off class membership limits are also reported. They define the distance of samples from each PCA class model; if a sample belongs to a predefined class it should lie within its boundaries. PLS regression is used to find the linear relationship between a set of independent variables (**X**) and a measured variable (**y**). This technique uses measured properties to construct models, often based on minimal differences between similar samples, that seek regularities in variable changes linked to the measured properties under study. The orthogonal variation of PLS (OPLS) separates the systematic variation in X into two parts, one part that is correlated (predictive) to **y** and the other is uncorrelated (orthogonal) to **y**.[17]

PrP^{Sc} quantification in brain

To determine the relative amount of PrP^{Sc} per μg in the whole brain of asymptomatic and clinically scrapie sick sheep, we compared the intensity of the WB signals of each brain to a standard curve generated from WB signals of serial naturally scrapie-infected brain dilutions. For this purpose, we used a WB procedure in which the quantification of the total loaded brain proteins was performed using the BCA Protein Assay Kit (23-225 BCA™ Protein Assay Kit, Pierce) and the intensity of the WB signals of the typical PrP^{Sc} bands was captured and quantified by densiometric analysis using a Chemidoc Imager System (BioRad).[18]

Ethics statement

The protocol used for the slaughtering procedures involving the sheep investigated herein was officially approved by the Service for Animal Welfare of the Istituto Zooprofilattico Sperimentale della Sardegna according to the guidelines no. I 09 044, in tight agreement with the guidelines of Italian National Law no. 116/1992. Sheep were humanely euthanized with a barbiturate solution, followed by injection of 4 mL of embutramide and mebenzonic iodide (Hoechst Roussel Vet, Italy).

We declare that the study was carried out on private animals under the request of the owners and all sheep were institutionally examined in the framework of the scrapie surveillance plan, and thereby no permission from an ethics committee was needed. The Istituto Zooprofilattico Sperimentale della Sardegna has been commissioned by the Italian Health Ministry to carry out all the analysis related to the regional scrapie surveillance plan.

Results

^{1}H NMR experiments

The ^{1}H NMR technique was applied to study the brain metabolite profile of infected and healthy sheep. The ^{1}H NMR spectra of the aqueous phase of brain extracts are characterized by sharp peaks assigned to the functional groups of low molecular weight metabolites found in a free state. A representative ^{1}H NMR spectrum of the brain extract is shown in Fig. 1, where it has been divided into two main spectral regions having different intensities. The first, Fig. 1A, from 0.5 to 5.0 ppm, contains signals from the aliphatic groups of free amino acids and derivatives, including the three branched chain amino acids (BCAA: valine, leucine, and isoleucine), glutamine (Gln), alanine (Ala), aspartate (Asp), *N*-acetyl aspartate (NAA), gamma-aminobutyric acid (GABA), and taurine (Tau); signals of organic acids such as lactate (Lac) and acetate (Ace), the trimethylamine group of choline and choline-containing compounds: 3-*glycero*-phosphocholine/phosphocholine (Chol), *myo*-inositol (MI), and creatine (Crt). In the spectral portion between 5.5 and 9.0 ppm, Fig. 1B, resonating less intense signals, attributed to the aromatic protons of amino acids such as tyrosine (Tyr), phenylalanine (Phe), and of nucleosides and nucleobases such as uracil (Ura), cytosine (Cyt), inosine (Ino), and hypoxanthine (Hyp); of nicotinamide adenine dinucleotide (NAD), formate (Form) and fumarate (Fum). Other detected NMR peaks were not unambiguously identified, also due to the possible loss of information, linked to the ^{2}H exchange of labile protons.[19] Once the spectra were fully assigned, the areas representative of the most relevant metabolites were measured by means of spectral area integration. Due to the intrinsic nature of ^{1}H NMR spectroscopy to detect, in principle, all hydrogen atoms in a molecule, excluding the fast changing ones, several metabolites, such as MI, exhibit resonances in different regions of the spectrum; taking into consideration this observation, areas to be integrated, diagnostic of a single metabolite, were carefully chosen among those being not overlapped and baseline well resolved. The results are reported in Table 1. Seldom, when 3 different extracts of the same brain were examined, quantitative differences of NAA and its hydrolysis products *N*-Ace (*N*-acetyl) and Asp were observed. Quantitative analysis of the 3 compounds indicated that, to a certain extent, hydrolysis of NAA has taken place[20,21] during sample handling. Considering the reported relevance of NAA in brain diseases[5,22] not to lose this

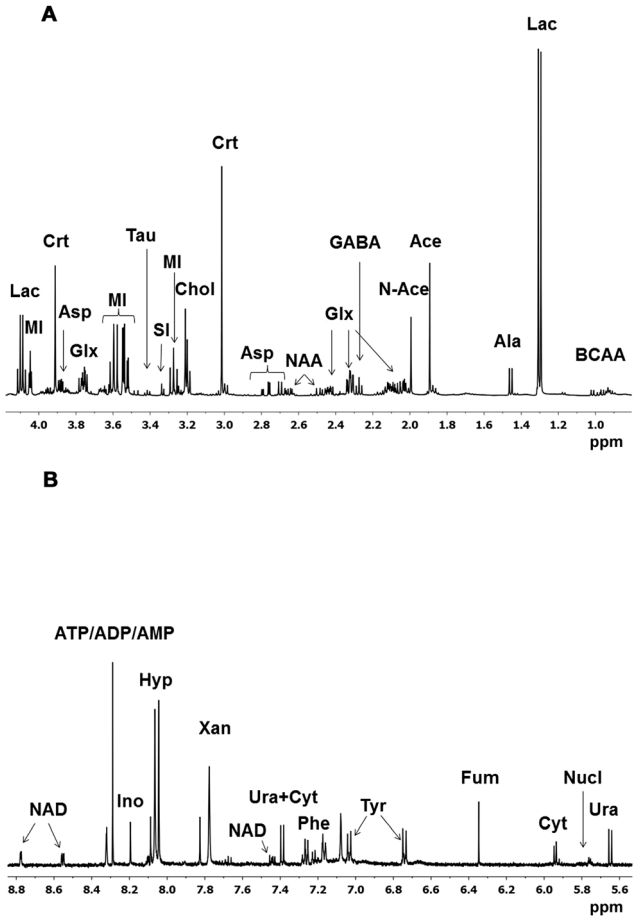

Fig. 1 A representative ^{1}H NMR spectrum of brain extract. (A) The spectral region from 0.5 to 5.0 ppm and (B) the spectral region from 5.5 to 9.0 ppm (magnified). Major assignments are reported. Branched chain amino acids: isoleucine, leucine, and valine (BCAA), lactate (Lac), alanine (Ala), acetate (Ace), *N*-acetyl groups (*N*-Ace), gamma-aminobutyric acid (GABA), glutamate/glutamine (Glx), *N*acetylaspartate (NAA), aspartate (Asp), creatine (Crt), choline/phosphocholine/3-*glycero*-phosphocholine (Chol), taurine (Tau), *myo*-inositol (MI), *scyllo*-inositol (SI), cytosine (Cyt), nucleosides (Nucl), uracil (Ura), fumarate (Fum), tyrosine (Tyr), phenylalanine (Phe), xanthine (Xan), hypoxanthine (Hyp), inosine (Ino), ATP/ADP/AMP (AP), and NAD.

information and, on the other hand, to overcome this bias, these molecular components were considered as unique variables, and therefore NAA (2.67–2.65 ppm) and Asp (2.83–2.76 ppm) normalized integrals were summed up and the new variable was named Asp-tot; analogously, Ace-tot was obtained by summing up *N*-Ace (singlet at 2.01 ppm) and Ace (singlet at 1.91 ppm) integrals. Following these procedures for each brain, a total of 24 variables (reported as means over 3 extracts) ready for MVA were obtained.

Data set overview by PCA

At a glance, no spectral differences were detectable between the ^{1}H NMR spectra of healthy and infected symptomatic as well as asymptomatic brain extracts. To extract the information, in terms of similarities and dissimilarities of samples based on the metabolite characteristics, contained in the set of spectra, a PCA of the spectral data (20 samples and 24 variables) was performed. The first two PCs described 59% of the variance and no outliers were detected. From the analysis of the score plot PC1 *vs.* PC2, shown in Fig. 2, it can be seen that S samples lie, although scattered in two groups, on the left side of the plot, while H and A samples, that tend to cluster, are projected on the right side. The results of this unsupervised analysis showed that the healthy and infected brains had different metabolite profiles, and that A brain samples shared common features with the H ones.

Table 1 Selected spectral regions and assigned metabolites used for this study

Metabolites (abbreviations)	Functional group[a]	Multiplicity[b]	Range[c] (ppm)
BCAA[d]	$-CH_3$	m	1.06–0.89
Alanine (Ala)	$-CH_3$	s	1.49–1.46
Acetate (Ace)	$-CH_3$	s	1.91
N-Acetyl groups (*N*-Ace)	$-CH_3$	s	2.01
GABA	$-\beta CH_3$		2.32–2.27
Glutamate (Glu)	$-\gamma CH_2$	m	2.37–2.32
Glutamine (Gln)	$-\gamma CH_2$	m	2.48–2.42
N-Acetyl aspartate (NAA)	$-\beta CH_2$	dd	2.67–2.65
Aspartate (Asp)	$-\beta CH_2$	dd	2.83–2.76
Choline[e] (Chol)	$-N(CH_3)_3$	s	3.25–3.19
Scyllo-inositol (SI)	–CH	s	3.37–3.33
Taurine (Tau)	$S-CH_2$	t	3.46–3.41
Creatine (Crt)	$N-CH_2$	s	3.95–3.92
Myo-inositol (MI)	–C2H	t	4.09–4.04
Lactate (Lac)	–CH	q	4.15–4.08
Uracil (Ura)	–C5H	d	5.83–5.79
Nucleosides (Nucl)	–C3H, –C5H	d	5.94–5.90
Cytosine (Cyt)	–C5H	d	6.12–6.09
Fumarate (Fum)	$-(CH)_2$	s	6.51
Tyrosine (Tyr)	–C3H, –C5H	d	6.92–6.88
Phenylalanine (Phe)	–C3H, –C4H, –C5H, –C6H	m	7.45–7.31
Xanthine (Xan)	–CH	s	7.94
Hypoxanthine (Hyp)	–CH	s	8.28–8.17
Inosine (Ino)	–CH	s	8.36
ATP/ADP/AMP (AP)	–CH	s	8.45
NAD	–C6H	d	8.75–8.68
NAD	–C8H	s	8.96–8.90

[a] The molecule numbering system follows IUPAC rules. [b] s = singlet, d = doublet, t = triplet, m = multiplet. [c] ppm with respect to TSP. [d] Branched chain amino acids. [e] Choline and choline-containing compounds.

Discriminant analysis for metabolite identification of H *vs.* S samples

The results of the PCA showed that the H and S samples had different metabolite profiles and that the S samples presented a higher intra-class variability. To find the metabolites that discriminate the different classes of samples an OPLS-DA was performed on 2 sample classes, H *vs.* S. This produced a 2-component validated model with R^2Y = 0.94 and Q^2 = 0.89, indicating a good fitting and a good classification power. Loading values along the predictive component were studied to attribute discriminant metabolites to each class. The results are reported in Table 2, where only the most important metabolites, *i.e.* those having the highest loading values that indicate a higher importance (weight) of the variable in discriminating the sample class, are reported. The most discriminant variables were

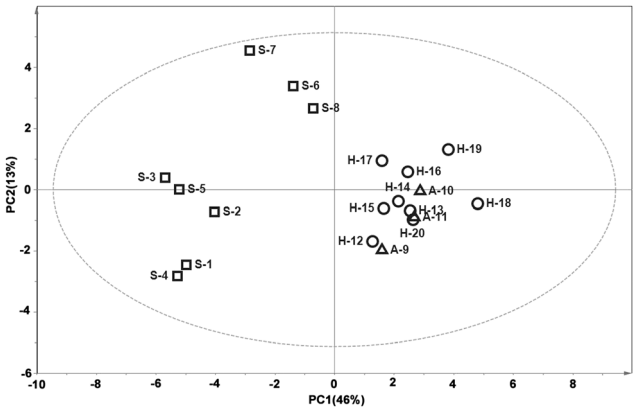

Fig. 2 PCA of spectral data of brain extracts. PCA of ^{1}H NMR spectral data of brain extracts, the PC1 *vs.* PC2 score plot of S (boxes), H (circles), and A (triangles) samples. The explained variance is reported in brackets. The ellipse encloses the 95% Hotelling T^2 confidence region.

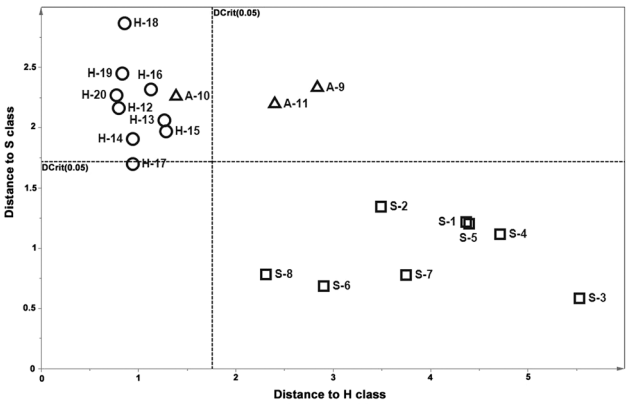

Fig. 3 Cooman's plot of spectral data of brain extracts. SIMCA Cooman's plot. In the *x*-axis PCA of H samples: 47% of the total variance expressed, 2 components; in the *y*-axis PCA of S samples: 65% of the total variance expressed, 2 components for S. The plot is divided into four regions by the intersection of 95% confidence limit lines for each class. These regions identify the class membership: the NW region defining H only, the SE region defining S only, the SW region containing both H and S, and the NE region containing neither H nor S membership.

found to be Ino, Cyt, Crt, and Lac, up regulated in S samples, while Asp-tot, GABA, Tyr, Ura, Phe, and BCAA were down regulated.

Characterization of A samples

The PCA score plot of Fig. 2 shows that H and A samples are clustered. For a deeper investigation of the characteristics of A samples, although numerically very limited, we performed further MVA. SIMCA was used for predicting the class belonging to A samples with regard to H and S classes and the results visualized in the Cooman's plot are reported in Fig. 3, where the multivariate spaces pertinent to H and S classes are shown. This showed that all the S and H samples were placed in their class membership zone. One (A10) out of the 3 infected asymptomatic samples projected into this space was classified as healthy, while the remaining 2, as not lying within the boundaries of any of the 2 (H and S) predefined classes, were classified to neither of the 2 classes.

With the aim of finding the metabolites that characterize the A class of samples we performed and cross-compared the results of two pairwise OPLS-DA models: "H *vs.* A" and "H *vs.* S", which were satisfactorily validated (R^2Y = 0.97 and Q^2Y = 0.62; R^2Y = 0.94 and Q^2Y = 0.89, respectively). The results, in terms of loading values, are shown as the SUS plot (Fig. 4). It is clearly visible that Chol is the variable that mostly characterizes the A samples. It is worth reminding that Chol variable comprises metabolites predominantly involved in the choline phospholipid metabolism (choline, phosphocholine and glycerol phosphocholine).[12] The two classes of infected samples (S and A) shared the metabolite Ino. Metabolites up regulated in A samples are reported in Table 2.

Table 2 OPLS-DA of the most discriminant metabolites of S and A classes compared to those of H class

	Classes	
Metabolites	S	A
Ino[a]	↑[b]	↑
Chol	—	↑
Asp-tot	↓	↓
GABA	↓	↑
Lactate	↑	↑
BCAA	↓	↓
Cyt	↑	—
Phe	↓	—
Tyr	↓	—
Crt	↑	—
Uracil	↓	—
Ala	↑	↑
Fum	—	↓

[a] Inosine (Ino), choline/phosphocholine/3-*glycero*-phosphocholine (Chol), aspartate + *N*-acetylaspartate (Asp-tot), gamma-aminobutyric acid (GABA), lactate (Lac), BCAA (branched chain amino acids: isoleucine, leucine, and valine), cytosine (Cyt), phenylalanine (Phe), tyrosine (Tyr), creatine (Crt), uracil (Ura), alanine (Ala), fumarate (Fum). [b] ↑ up-regulated, ↓ down-regulated, and — stable, with respect to the H class.

PrP^{sc} amounts and correlation with spectral data by PLS regression

The WB analysis, applied to the brain samples of infected symptomatic and asymptomatic sheep, revealed the same PrP^{Sc} molecular signature, thus suggesting that the same scrapie agent was involved in all the examined affected sheep. PrP^{Sc} deposition was demonstrated in all the examined brains of S and A sheep and data are reported in Table 3 and Fig. 5. The PrP^{Sc} amounts were generally higher in the S sheep compared to those in A sheep although Student's *t*-test indicated that means are not statistically different. To ascertain whether the metabolite profile of brains is linked to PrP^{sc} quantities, we performed an OPLS regression on NMR data with PrP^{sc} amount as response. The quality of the OPLS regression model was highly satisfactory (1 + 2 components, R^2Y = 0.997 and Q^2Y = 0.87), thus indicating that there were modifications in the metabolite profile strongly linearly linked to PrP^{sc} amount. In Table 4, we report the metabolites having the strongest (either positive or

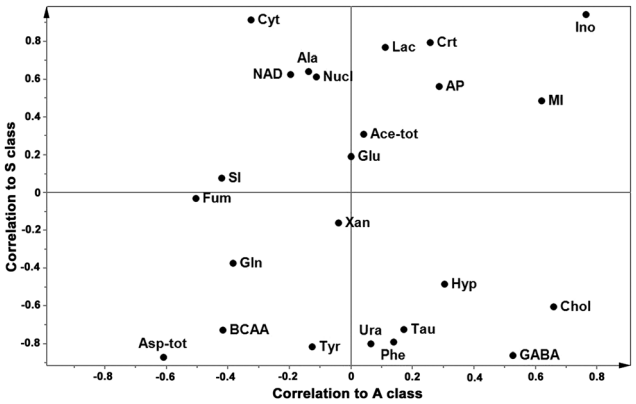

Fig. 4 SUS plot of spectral data of brain extracts. The loading SUS-plot of OPLS-DA models of ^{1}H NMR data of brain extracts. The *x*-axis represents the loading correlation values of the "H *vs.* A" model and the *y*-axis represents the loading correlation values of the "H *vs.* S" model. Variables in the lower left corner are unique for H samples and variables in the higher right corner are shared in infected (S and A) samples. Variables higher in S and A samples exhibit high correlation values in the *y*- and *x*-axes, respectively. Branched chain amino acids: isoleucine, leucine, and valine (BCAA), lactate (Lac), alanine (Ala), acetate + *N*-acetyl groups (Ace-tot), gamma-aminobutyric acid (GABA), glutamate (Glu), glutamine (Gln), aspartate + *N*-acetylaspartate (Asp-tot), creatine (Crt), choline/phosphocholine (Chol), taurine (Tau), myo-inositol (MI), scyllo-inositol (SI), cytosine (Cyt), nucleosides (Nucl), uracil (Ura), fumarate (Fum), tyrosine (Tyr), phenylalanine (Phe), xanthine (Xan), hypoxanthine (Hyp), inosine (Ino), ATP/ADP/AMP (AP), and NAD.

Table 3 PrP^{Sc} amounts[a], as calculated by WB analysis in brains of infected sheep

Sample	Density (OD mm^{-2})
Infected symptomatic	
S-1	181.89
S-2	130.02
S-3	223.09
S-4	198.06
S-5	187.92
S-6	176.35
S-7	204.60
S-8	167.03
Mean	183.62
SD	27.85
Infected asymptomatic	
A-9	104.26
A-10	171.93
A-11	124.01
Mean	133.40
SD	34.79

[a] Means are not statistically different.

negative) correlation with PrP^{sc} levels. The results of *t*-test on Ala data of infected and healthy samples reject the null hypothesis at $p > 0.05$.

Discussion and conclusions

Our results indicated that clinically scrapie affected sheep have different brain metabolite profiles compared to the healthy ones, while the asymptomatic affected animals, although more similar to the healthy group, have also their own metabolite features. To our knowledge, this is the first metabonomic study performed in naturally infected sheep with scrapie.

In this study, although the number of the sheep considered is relatively small, assessing the metabolite profile in the whole brain using ^{1}H NMR and different MVA techniques, we found different metabolite profiles in H, S, and A sheep. As results from the OPLS-DA "S *vs.* H" and as shown in the SUS plot, Ino is the metabolite having a relatively higher level in the infected sheep (S and A) when compared with the healthy ones. Cyt, Crt, and Lac are discriminant of S samples, and as we can see in the SUS-plot, choline and choline-containing compounds (phosphocholine and glycerol phosphocholine) characterized the A samples. Healthy brains were characterized by relatively high levels of BCAA, Phe, Ura, Tyr, GABA, and Asp-tot. It is interesting to note that, correlating the metabolite profiles to the PrP^{Sc} amounts, Ala was the most important metabolite, having the strongest positive correlation with PrP^{Sc} amounts. GABA, Ura, and Asp-tot were the metabolites that inversely correlated with both PrP^{Sc} levels and discriminated H samples.

We found a higher level of Lac in the extracts of S brains when compared to the H ones. It generally indicates a more intense anaerobic metabolism, which can be observed under hypoxic/anoxic stress conditions affecting the brains or other organs and can indicate ischemic processes and apoptosis. Although not significantly correlated with PrP^{sc} amounts, it can be hypothesized that the increase of Lac is a sign of general sickness but not specifically linked to the PrP^{sc} generation. Ino was found to be in a relatively high quantity in S and A brains: it is the breakdown product of ATP and is formed by deamination of adenosine, mainly at high intracellular concentrations, which are associated with hypoxia, ischemia and other forms of cellular stress.[23] Crt is higher in S brains and also correlated with PrP^{sc}. Crt is thought to have a multifaceted role in the brain. Besides being involved in brain osmoregulation, it has recently been implicated in energy homeostasis and direct antioxidant effects.[24,25] Furthermore, Crt plays an integral role in the cellular energy metabolism, and thus an increase in the concentration of this compound may be a result of metabolic stress. Dysregulation of Crt may implicate an energetic shift in the brain, suggesting an increased metabolic activity and/or a depletion of the energy storage capacity.[24,26] Crt has several potential neuroprotective effects,[25] including buffering intracellular mitochondrial energy reserves, stabilizing intracellular calcium, and inhibiting activation of the mitochondrial permeability transition pore, which have all been linked to apoptotic and oxidative cell death.[27] Asymptomatic samples are characterized by choline, phosphocholine and glycerol phosphocholine. Choline is an essential nutrient with a complex role in the body. It is required for synthesis of the neurotransmitter acetylcholine and of phosphatidylcholine, the major constituent of membranes.[11] It is also involved in cell-membrane signaling (phospholipids), lipid transport (lipoproteins), and the methyl group metabolism (homocysteine reduction).[28] In MRS, choline is a marker of the cellular membrane turnover, and is therefore

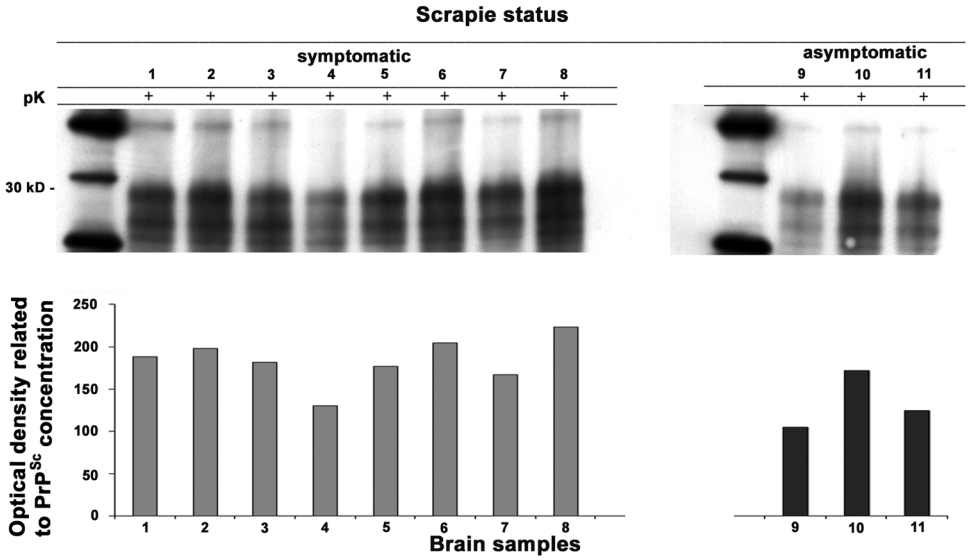

Fig. 5 Quantification of PrP^{Sc} in brain homogenates of naturally scrapie-affected sheep. (A) Western blot (WB) analysis of whole-brain homogenates from independent symptomatic (lines 2 to 9) and asymptomatic (lines 10 to 13) scrapie affected sheep after proteinase K (PK) digestion. A molecular weight marker is loaded in lane 1. (B) Quantification of the WB signal of the PrP^{Sc} present in the brain homogenates is represented as PrP optical density (OD) signals. Our results indicate that the higher average amount of PrP^{Sc} was detected in the symptomatic scrapie affected sheep. The brain homogenate samples were normalized in relation to the total protein amount.

Table 4 OPLS metabolites having the strongest (positive or negative) correlation with PrP^{sc} amounts in brain homogenates

Metabolites	r^a	$R^{2\,b}$	Loadings[c]	Loadings cv[d]
Directly correlated ↑				
Ala	0.861	0.742	0.327	0.099
Cyt	0.803	0.645	0.300	0.103
Crt	0.639	0.408	0.248	0.119
Inversely correlated ↓				
Asp-tot	−0.780	0.608	−0.302	0.162
Ura	−0.609	0.370	−0.237	0.183
GABA	−0.602	0.363	−0.218	0.102

[a] Coefficient of correlation. [b] Coefficient of determination of metabolite *vs.* PrP^{sc} amounts. [c] Loading weights along the predictive component. [d] Jack-knife standard error of loading weights computed from all rounds of cross validation. Alanine (Ala), cytosine (Cyt), creatine (Crt), aspartate + *N*-acetylaspartate (Asp-tot), uracil (Ura), gamma-aminobutyric acid (GABA).

elevated in neoplasms, demyelination and gliosis. Phosphocholine, which contributes to the choline resonance, may act as a biomarker for the membrane phospholipid metabolism/turnover.[29] Choline is also a constituent of sphingolipids that participate in the formation of the lipid rafts where the GPI protein is anchored. Naslavsky[30] reported that in neuroblastoma cells infected with prions, sphingolipid depletion increases the formation of PrP^{Sc}. Deregulation of sphingolipids metabolism in Alzheimer's disease has also been reported.[31] The choline biomarker in A brains could be an early sign of brain cellular membrane damage due to lipid raft formation and protein anchorage. Amino acids play important functions as neurotransmitters providing both excitatory and inhibitory stimuli. Here, we found that the levels of amino acid Asp-tot, Tyr, Phe and BCAA are lower in the brains of S sheep. This may be a consequence of the neurodegenerative phenomena affecting pre- and post-synaptic processes, a commune pattern observed in distinct brain regions when exposed to prion[32] or to beta-amyloid oligomers in Alzheimer's disease. The loss of a selective subpopulation of GABAergic neurons has been demonstrated in an experimentally prion infected mouse[33] by detecting glutamic acid decarboxylase, the GABA synthesizing enzyme, immunohistochemically. This correlates well with our observation of a lower level of GABA in the S brains when compared to H. Moreover, the lower GABA level seems to be relegated to the clinical stage of scrapie, as being not observed as discriminant in the asymptomatic sheep. In this respect, a decrease of the GABA activity has been observed at the clinical stage in scrapie infected hamster.[34] The Asp-tot (comprising NAA and Asp) level is lower in S and A sheep. The decrease of NAA is a finding that has been already described at earlier stages of the disease in the murine model after experimental prion infection.[6] NAA is an abundant metabolite which is present only in neurons in the adult brain, and although its role in the cell is little known, it is widely considered to be a marker of functional neurons.[6] A lower level of Ura has been observed in brains of symptomatic sheep when compared to the healthy ones. Although little is known about the neuronal functions of Ura, it has been suggested that it modulates many neurotransmitters or neuromodulators, especially in the mature central nervous system[35] and its glycosylated form, uridine, has been proposed as a neuroprotective agent in neurodegenerative disorders.[36] Ala was the metabolite more strongly linked to PrP^{sc} amounts in scrapie sheep brains. Ala has been indicated as a biomarker of apoptosis and/or cellular stress processes in brain, which are both normally observed in scrapie neuropathology.[37] In addition, the increase of Ala has also been observed in meningioma and following ischemia;[38] the concentration of plasma Ala was significantly increased ($p < 0.05$) in infected BSE dairy cattle as well.[39]

Among the biases that could affect the reliability of our results, the potential presence of different scrapie agent strains implicated in our cases should be taken into account. In general, neuropathological changes, including the PrP^{Sc} molecular signature and its regional distribution in the brain, are strictly related to the TSE agent strain involved and to the PrP genotype of the host; thus these differences related to the host might influence the ^{1}HMRS neuro-metabolic profile.[40] Our study has the advantage that all cases belong to the same flock, and only one identical molecular signature was found among the different cases examined. In addition, it is worth recalling that only one identical scrapie agent strain has been found in Italy so far.[41]

The approach described herein was able to identify different metabolite profiles pertaining to healthy and infected sheep brains, and physiopathological roles of metabolites mainly involved may explain their different expressions in these two extreme situations. Determining the metabolite modifications in the asymptomatic and symptomatic phases of the disease might clarify some of the molecular mechanisms of the prion disease and disease progression. As in previous studies, our findings confirm the close relationship between scrapie and other neurodegenerative diseases, although comparing ruminant brain metabolites to human brain metabolites can be, to some extent, hazardous. This study concerns *in vitro* analysis of the whole brain, although the widespread pathology onset has specific neuroanatomical locations; in this respect, future investigations will be dedicated to the study of metabolite fingerprints in different affected areas.

Funding

This study was supported by grants from the Regione Autonoma della Sardegna (L.R. no. 7/2007, call 2008).

Acknowledgements

We thank Prof. E. d'Aloja for helpful discussion and Dr M. G. Cancedda for sheep brain recruitments. D. Perra gratefully acknowledges the Sardinia Regional Government for the financial support of her PhD scholarship (P.O.R. Sardegna F.S.E. Operational Programme of the Autonomous Region of Sardinia, European Social Fund 2007–2013 – Axis IV Human Resources Objective l.3, Line of Activity l.3.1).

References

1 S. B. Prusiner, Prions, *Proc. Natl. Acad. Sci. U. S. A.*, 1998, **95**, 13363–13383.
2 O. Andréoletti, P. Berthon, D. Marc, P. Sarradin, J. Grosclaude, L. van Keulen, F. Schelcher, J. M. Elsen and F. Lantier, Early accumulation of PrPSc in gut-associated lymphoid and nervous tissues of susceptible sheep from a Romanov flock with natural scrapie, *J. Gen. Virol.*, 2000, **81**, 3115–3126.
3 L. J. van Keulen, B. E. Schreuder, M. E. Vromans, J. P. Langeveld and M. A. Smits, Pathogenesis of natural scrapie in sheep, *Arch. Virol., Suppl.*, 2000, **16**, 57–71.
4 T. M. Tsang, B. Woodman, G. A. McLoughlin, J. L. Griffin, S. J. Tabrizi, G. P. Bates and E. Holmes, Metabolic characterization of the R6/2 transgenic mouse model of Huntington's disease by high-resolution MAS ^{1}H NMR spectroscopy, *J. Proteome Res.*, 2006, **5**, 483–492.
5 E. Holmes, T. M. Tsang and S. J. Tabrizi, The application of NMR-based metabonomics in neurological disorders, *NeuroRx*, 2006, **3**, 358–372.
6 K. A. Broom, D. C. Anthony, J. P. Lowe, J. L. Griffin, H. Scott, A. M. Blamire, P. Styles, V. H. Perry and N. R. Sibson, MRI and MRS alterations in the preclinical phase of murine prion disease: association with neuropathological and behavioural changes, *Neurobiol. Dis.*, 2007, **26**, 707–717.
7 A. Rosa, P. Scano, A. Incani, F. Pilla, C. Maestrale, M. Manca, C. Ligios and A. Pani, Lipid profiles in brains from sheep with natural scrapie, *Chem. Phys. Lipids*, 2013, **175**, 33–40.
8 J. K. Nicholson, J. C. Lindon and E. Holmes, 'Metabonomics': understanding the metabolic responses of living systems to pathophysiological stimuli *via* multivariate statistical analysis of biological NMR spectroscopic data, *Xenobiotica*, 1999, **29**, 1181–1189.
9 C. Ligios, M. G. Cancedda, L. Madau, C. Santucciu, C. Maestrale, U. Agrimi, G. Ru and G. DiGuardo, $PrP^{(Sc)}$ deposition in nervous tissues without lymphoid tissue involvement is frequently found in ARQ/ARQ Sarda breed sheep preclinically affected with natural scrapie, *Arch. Virol.*, 2006, **151**, 2007–2020.
10 J. Folch, M. Lees and G. H. Sloane-Stanley, A simple method for the isolation and purification of total lipid from animals tissues, *J. Biol. Chem.*, 1957, **226**, 497–509.
11 V. Govindaraju, K. Young and A. A. Maudsley, Proton NMR chemical shifts and coupling constants for brain metabolites, *NMR Biomed.*, 2000, **13**, 129–153.
12 A. Viola, V. Saywell, L. Villard, P. J. Cozzone and N. W. Lutz, Metabolic fingerprints of altered brain growth, osmoregulation and neurotransmission in a Rett syndrome model, *PLoS One*, 2007, **2**(1), e157.
13 D. S. Wishart, C. Knox, A. C. Guo, R. Eisner, N. Young, B. Gautam, D. D. Hau, N. Psychogios, E. Dong, S. Bouatra, R. Mandal, I. Sinelnikov, J. Xia, L. Jia, J. A. Cruz, E. Lim, C. A. Sobsey, S. Shrivastava, P. Huang, P. Liu, L. Fang, J. Peng, R. Fradette, D. Cheng, D. Tzur, M. Clements, A. Lewis, A. De Souza, A. Zuniga, M. Dawe, Y. Xiong, D. Clive, R. Greiner, A. Nazyrova, R. Shaykhutdinov, L. Li, H. J. Vogel and I. Forsythe, HMDB: a knowledgebase for the human metabolome, *Nucleic Acids Res.*, 2009, **37**, 603–610.
14 P. Scano, A. Rosa, E. Locci, G. Manzo and M. A. Dessì, Modifications of the ^{1}H NMR metabolite profile of processed mullet (*Mugil cephalus*) roes under different storage conditions, *Magn. Reson. Chem.*, 2012, **50**, 436–442.
15 M. Bylesjö, M. Rantalainen, O. Cloarec, J. K. Nicholson, E. Holmes and J. Trygg, OPLS discriminant analysis: combining the strengths of PLS-DA and SIMCA classification, *J. Chemom.*, 2006, **20**, 341–351.

16 S. Wiklund, E. Johansson, L. Sjöström, E. J. Mellerowicz, U. Edlund, J. P. Shockcor, J. Gottfries, T. Moritz and J. Trygg, Visualization of GC/TOF-MS-Based Metabolomics Data for Identification of Biochemically Interesting Compounds Using OPLS Class Models, *Anal. Chem.*, 2008, **80**, 115–122.

17 L. Eriksson, E. Johansson, N. Kettaneh-Wold, J. Trygg, C. Wikstrom and S. Wold, *Multi-and Megavariate Data Analysis*, Umetrics Academy, Sweden, 3rd edn, 2013.

18 C. Ligios, G. M. Cancedda, I. Margalith, C. Santucciu, L. Madau, C. Maestrale, M. Basagni, M. Saba and M. Heikenwalder, Intraepithelial and interstitial deposition of pathological prion protein in kidneys of scrapie-affected sheep, *PLoS One*, 2007, **2**(9), e859.

19 F. Commodari, D. L. Arnold, B. C. Sanctuary and E. A. Shoubridge, ^{1}H NMR characterization of normal human cerebrospinal fluid and the detection of methylmalonic acid in a vitamin B12 deficient patient, *NMR Biomed.*, 1991, **4**, 192–200.

20 E. M. Ratai, S. Pilkenton, M. R. Lentz, J. B. Greco, R. A. Fuller, J. P. Kim, J. He, L. L. Cheng and R. G. González, Comparisons of brain metabolites observed by HRMAS ^{1}H NMR of intact tissue and solution ^{1}H NMR of tissue extracts in SIV-infected macaques, *NMR Biomed.*, 2005, **18**, 242–251, DOI: 10.1002/nbm.953.

21 J. R. Moffett, P. Arun, P. S. Ariyannur and A. M. Namboodiri, N-Acetylaspartate reductions in brain injury: impact on post-injury neuroenergetics, lipid synthesis, and protein acetylation, *Front. Neuroenerg.*, 2013, **5**, 1–19.

22 M. H. Baslow, N-acetylaspartate in the vertebrate brain: metabolism and function, *Neurochem. Res.*, 2003, **28**, 941–953.

23 G. Haskó, M. V. Sitkovsky and C. Szabo, Immunomodulatory and neuroprotective effects of inosine, *Trends Pharmacol. Sci.*, 2004, **25**, 152–157.

24 M. R. Pears, J. D. Cooper, H. M. Mitchison, R. J. Mortishire-Smith, D. A. Pearce and J. L. Griffin, High resolution ^{1}H NMR-based metabolomics indicates a neurotransmitter cycling deficit in cerebral tissue from a mouse model of Batten disease, *J. Biol. Chem.*, 2005, **280**, 42508–42514.

25 W. Zhang, M. Narayanan and R. M. Friedlander, Additive neuroprotective effects of minocycline with creatine in a mouse model of ALS, *Ann. Neurol.*, 2003, **53**, 267–270, DOI: 10.1002/ana.10476.

26 M. J. Lan, G. A. McLoughlin, J. L. Griffin, T. M. Tsang, J. T. J. Huang, P. Yuan and S. Bahn, Metabonomic analysis identifies molecular changes associated with the pathophysiology and drug treatment of bipolar disorder, *Mol. Psychiatry*, 2008, **14**, 269–279.

27 S. J. Tabrizi, A. M. Blamire, D. N. Manners, B. Rajagopalan, P. Styles, A. H. Schapira and T. T. Warner, Creatine therapy for Huntington's disease: clinical and MRS findings in a 1-year pilot study, *Neurology*, 2003, **61**(1), 141–142.

28 S. H. Zeisel and K. A. Da Costa, Choline: an essential nutrient for public health, *Nutr. Rev.*, 2009, **67**(11), 615–623.

29 R. Senaratne, A. M. Milne, G. M. MacQueen and G. B. Hall, Increased choline-containing compounds in the orbitofrontal cortex and hippocampus in euthymic patients with bipolar disorder: a proton magnetic resonance spectroscopy study, *Psychiatry Res., Neuroimaging*, 2009, **172**, 205–209.

30 N. Naslavsky, H. Shmeeda, G. Friedlander, A. Yanai, A. H. Futerman, Y. Barenholz and A. Taraboulos, Sphingolipid depletion increases formation of the scrapie prion protein in neuroblastoma cells infected with prions, *J. Biol. Chem.*, 1999, **274**(30), 20763–20771.

31 X. He, Y. Huang, B. Li, C. X. Gong and E. H. Schuchman, Deregulation of sphingolipid metabolism in Alzheimer's disease, *Neurobiol. Aging*, 2010, **31**, 398–408.

32 Z. Siskova, R. A. Reynolds, V. O'Connor and V. H. Perry, Brain region specific pre-synaptic and post-synaptic degeneration are early components of neuropathology in prion disease, *PLoS One*, 2013, **8**(1), e55004, DOI: 10.1371/journal.pone.0055004.

33 M. Guentchev, M. H. Groschup, R. Kordek, P. P. Liberski and H. Budka, Severe, early and selective loss of a subpopulation of GABAergic inhibitory neurons in experimental transmissible spongiform encephalopathies, *Brain Pathol.*, 1998, **8**, 615–623.

34 J. M. Durand-Gorde, J. Bert and A. Nieoullon, Early changes in tyrosine hydroxylase, glutamic acid decarboxylase and choline acetyltransferase golden hamster striatum after intracerebral inculation of the nigrostriatal system with scrapie agent (263 K), *Neurosci. Lett.*, 1984, **51**, 37–42.

35 D. Lecca and S. Ceruti, Uracil nucleotides: From metabolic intermediates to neuroprotection and neuroinflammation, *Biochem. Pharmacol.*, 2008, **75**, 1869–1881, DOI: 10.1016/j.bcp.2007.12.009, ISSN 0006-2952.

36 A. Dobolyi, G. Juhasz, Z. Kovacs and J. Kardos, Uridine function in the central nervous system, *Curr. Top. Med. Chem.*, 2011, **11**, 1058–1067.

37 H. M. Schätzl, L. Laszlo, D. M. Holtzman, J. Tatzelt, S. J. DeArmond, R. I. Weiner, W. C. Mobley and S. B. Prusiner, A hypothalamic neuronal cell line persistently infected with scrapie prions exhibits apoptosis, *J. Virol.*, 1997, **71**, 8821–8831.

38 S. N. Reinke, B. H. Walsh, G. B. Boylan, B. D. Sykes and L. C. Kenny, *et al.*^{1}H NMR derived metabolomic profile of neonatal asphyxia in umbilical cord serum: implications for hypoxic ischemic encephalopathy, *J. Proteome Res.*, 2013, **12**, 4230–4239.

39 G. G. Allison, R. A. Horton, P. Rees Stevens, R. Jackman and J. M. Moorby, Changes in plasma metabolites and muscle glycogen are correlated to bovine spongiform encephalopathy in infected dairy cattle, *Res. Vet. Sci.*, 2008, **80**, 40–46, DOI: 10.1016/j.rvsc.2006.11.008.

40 R. Lodi, P. Parchi, C. Tonon, D. Manners, S. Capellari, R. Strammiello, R. Rinaldi, C. Testa, E. Malucelli, B. Mostacci, G. Rizzo, G. Pierangeli, P. Cortelli, P. Montagna and B. Barbiroli, Magnetic resonance diagnostic markers in clinically sporadic prion disease: a combined brain magnetic resonance imaging and spectroscopy study, *Brain*, 2009, **132**, 2669–2679.

41 R. Nonno, E. Esposito, G. Vaccari, M. Conte, S. Marcon, M. Di Bari, C. Ligios, G. Di Guardo and U. Agrimi, Molecular analysis of cases of Italian sheep scrapie and comparison with cases of bovine spongiform encephalopathy (BSE) and experimental BSE in sheep, *J. Clin. Microbiol.*, 2003, **41**, 4127–4133.